*Journal of Harbin Engineering University*
*ISSN: 1006-7043*

Vol 47 No. 08
Aug 2026

# Improved Performance of t-SNE Feature-Based Convolutional Neural Network for Multi-Stage Alzheimer's Disease Detection

**Pawan Kumar Singh[1], Pawan Kumar Upadhyay[2]**
Department of Computer Science and Engineering
Jaypee Institute of Information Technology, Noida

**Abstract**
Alzheimer's is one of the most common causes of dementia, causing memory loss, impaired problem-solving skills, and other cognitive impairments that can interfere with daily functioning. Early detection is critical for timely intervention and for improving the patient's quality of life. Our proposed approach, structured into three distinct phases, has the potential to improve the detection of multi-stage Alzheimer's disease. In the first phase, to improve the quality and consistency of MRI images, various pre-processing steps are applied; furthermore, a deep synthetic oversampling technique is used to address class imbalance, thereby reducing bias and stabilizing variance across the dataset. This technique ensures a more uniform distribution of balanced samples across various Alzheimer's classes. In the second phase, t-distributed stochastic neighbor embedding is used to map high-dimensional class-sample representations into a lower-dimensional space, enabling clear visual examination of class separability. This helps to generate well-distributed clusters. In the third phase, the proposed convolutional neural network comprises four blocks to effectively extract meaningful anatomical structural features associated with grey-white matter organization, followed by a dense layer, which is critical for detecting subtle and advanced neurodegenerative disease. As a result of this proposed model evaluation, the accuracy improved to 97.97%, with corresponding improvements in precision, recall, and F1-score.

**Keywords**: Alzheimer's disease neuroimaging initiative dataset, adaptive moment estimation, convolutional neural network, t-distributed stochastic neighbor embedding.

## 1. Introduction

As a neurological disorder, Alzheimer's disease (AD) results in persistent memory loss, mental decline, and intellectual impairment. The most common cause of cognitive decline associated with dementia. Consequently, daily functioning continues to deteriorate [1]. The death of neurons is followed by the formation of amyloid plaques, neurofibrillary tangles, and eventual atrophy of brain tissue [1, 2], as reported by the World Health Organization [3]. By the year 2030, the number of people suffering from dementia is projected to increase to 78 million, and by 2050, it will reach 139 million, more than twice the number by 2021. It is common for individuals aged 65 years and older to have a high chance of developing dementia. However, young people have only a 3% probability of developing early-onset dementia [4]. In cases of delayed treatment, brain cells responsible for cognitive and memory functions are likely to be damaged, resulting in loss of brain function, reduced cognitive skills, language difficulties, and impaired logical thinking. The acute stage of dementia is caused by an inability to perform basic activities as a result of progressive degeneration of nerve cells. Therefore, early diagnosis of AD is extremely vital since it progresses over time. Alzheimer's disease is diagnosed using two procedures: (1) when symptoms appear and (2) through neuroimaging techniques. AD occurs before symptoms appear. It is classified as "preclinical AD" when neither the person nor those around them can observe any symptoms [5]. As a result of current imaging technologies, amyloid beta deposition, a marker of Alzheimer's, can be detected independent of symptoms [6]. It could prove useful for future clinical trials and AD treatments. Figure 1 [7] shows a comparison between an AD brain and a normal brain.

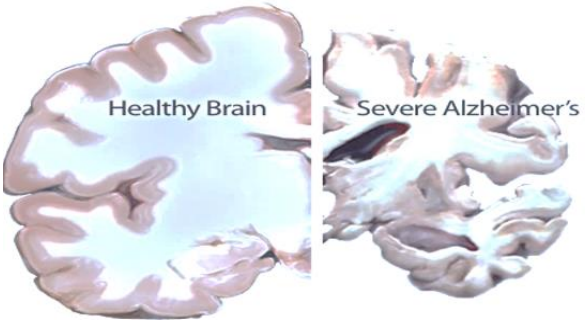


**Figure 1. Healthy brain and severe Alzheimer's brain [7].**

Despite this, modern imaging techniques are the most effective way to detect AD because they provide a non-invasive, internal view of the body. In the study of AD therapy, the most challenging period was when AD was only detected after death. In recent years, medical imaging devices have become increasingly important in detecting and treating Alzheimer's disease [8]. Furthermore, numerous neuroimaging techniques, such as MRI, help detect brain disorders in many cases. Although image data is the most appropriate dataset for detecting AD, handwritten data and drawing task datasets are also useful [9]. In the field of computer science, deep learning models can detect brain structure anomalies that are difficult to detect with MRI scans, analyze the progression of AD, and provide reliable results [10]. As a result, deep learning models like convolutional neural networks are ideal for analyzing two-dimensional images, but they can also be used with one-dimensional images and three-dimensional ones. To perform well, deep neural networks require a large amount of data [11].

The Alzheimer's data used in this paper is collected from the Alzheimer's Disease Neuroimaging Initiative, which contains 6400 MRI images of 2D slices. The dataset is divided into two stages, namely the training stage and the testing stage, and 80% will be allocated to the training stage and 20% to the testing stage. Various pre-processing techniques are used to improve image quality, such as resizing, color transformations, and anatomical features enhancement, followed by a deep synthetic oversampling method to balance the distribution of class samples across various Alzheimer's disease and avoid the class imbalance problem. Using this method, reduce bias and increase variance by augmenting the class-sample distribution to make it more balanced across minority classes.

Furthermore, t-Distributed Stochastic Neighbor Embedding enables visual assessment of class separability by projecting high-dimensional MRI features into a low-dimensional space. Finally, a convolutional neural network is proposed with two major components: a convolutional layer and a dense head. The convolutional layer extracts the anatomical features, while the dense head detects multi stage Alzheimer's disease.

This paper is organized as follows. Sect. 1: Introduction to Alzheimer's disease. Sect. 2 extends the related work on Alzheimer's disease. Sect.3 details the Alzheimer's Disease Neuroimaging Initiative dataset. Sect. 4 discusses the proposed approach to improving the detection of Alzheimer's disease. Sect.5 Discusses the obtained results of Alzheimer's disease detection. Sect. 6 summarizes the conclusion and highlights promising opportunities for the future in this area.

## 2. Related work

This section examines the recent advances in artificial intelligence and deep learning that have enabled the detection of AD at various stages of its progression. To address the drawbacks of conventional CNN-based methods, the author [12] proposed a novel deep learning approach for early detection of Alzheimer's disease. A depth-separable CNN backbone is integrated with multiple features and skip connections in the new approach to create an Improved Spatial Attention Block (I-SAB), which produces more informative spatial attention maps. Additionally, multilayer attention enhances robustness by producing scale-invariant features. Based on analysis of the OASIS and AD Datasets, the model achieved 99.75% and 96.20% accuracy, respectively, and achieved 83.25% accuracy in a domain adaptation test, demonstrating strong generalization. In another paper by the author [13], machine-learning accuracy is compared with model explainability when detecting Alzheimer's disease early. A trade-off between model explainability and machine-learning accuracy is highlighted in this paper about early detection of Alzheimer's disease. A support vector machine (SVM) was trained on 169,408 records with 1024 features, collected from the National Alzheimer's Coordinating Center. It achieved 88% (binary) and 72.8% (multiclass) for predicting AD progression over four years, with F1 scores of 98.9% and 90.7%, respectively. One more related paper, author [14], proposes an ensemble of Vision Transformers for AD classification, demonstrating its effectiveness in dealing with class imbalance and long-range dependencies. An ensemble of four vanilla ViTs, with soft and hard voting, was evaluated on the OASIS and ADNI datasets. By 4.14% and 4.72%, respectively, it outperformed machine learning models and CNNs. This paper demonstrates the effectiveness of the VIT model in situations where data is scarce and imbalanced, and provides open-source code to ensure reproducibility. An Inception-CNN hybrid model was proposed by the authors [15] for Alzheimer's disease detection. Using 6400 MRIs collected from ADNI, SMOTE-ENN enriches the dataset to improve the model's performance,

achieving 93.31% accuracy. The model outperforms state-of-the-art models in terms of accuracy, precision, recall, and F-score. Another paper connected, author [16] evaluated multiple transfer learning models, including VGG-19, Wide ResNet-50-2, GoogleNet, and Inception V3, using a Kaggle four-class Alzheimer MRI dataset, consisting of non-demented, very mild, mild, and moderately demented individuals. An ensemble method was proposed that integrated the decision outputs from these base classifiers and generated final predictions via fuzzy ranking based on the Gompertz function. The ensemble model achieved high performance on public MRI data, with 99.22% accuracy, 99.53% recall, 99.69% precision, a 99.61% F1-score, and an AUC of 98%, outperforming all individual models. In addition, the author [17] proposes using a convolutional neural network to detect Alzheimer's disease. This model uses a neural network–based multiclass classifier to extract shape and texture features from brain MRI scans to detect Alzheimer's disease. Due to its high accuracy, the proposed method is more effective at detecting Alzheimer's disease than conventional methods. According to another paper [18], MRI images from the Kaggle dataset are used to detect and classify Alzheimer's disease stages using a hybrid deep learning model combining VGG19 with additional layers and a CNN architecture. Compared with a standalone CNN, the proposed hybrid approach achieves superior accuracy, reaching 95.52% for Alzheimer's stage classification. In addition, the author proposed a novel framework [19] for integrating models for structured data analysis as well as MRI analysis. Structured data is captured with an LSTM network, and static features are learned using a feedforward neural network. MRI, on the other hand, uses ResNet50 and MobileNetV2 for spatial feature extraction. Data were collected from NACC and ADNI and compared with previous approaches. A hybrid multimodal model achieved 99.82% accuracy on the ADNI dataset and 96.19% on the NACC dataset, significantly outperforming previous methods.

## 3. Dataset

The Alzheimer's disease data were obtained from [15, 20, 21], which comprise 2D MRI slices of size (176 × 208) and as a part of the Alzheimer's Disease Neuroimaging Initiative [22], as shown in Figure 2.

**Figure 2.** MRI Samples of Alzheimer's dataset.

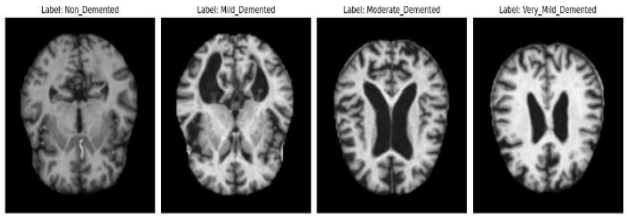


In neurology, the Alzheimer's Disease Assessment Scale [23] is used to assess disease severity. Severity ranges from 0 to 5 (0 = no impairment, 1 = very mild, 2 = mild, 3 = moderate, 4 = moderately severe, 5 = severe), and Figure 3 shows the distribution of MRI samples class-wise.

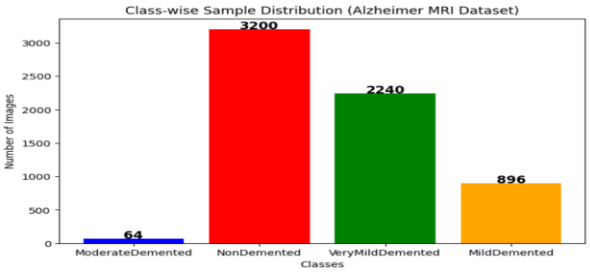


**Figure 3.** Distribution of Alzheimer's dataset.

## 4. Methodology

This section presents a proposed approach that efficiently detects Alzheimer's disease. This proposal describes three of the phases:

1. In the first phase, to enhance the quality, clarity, and uniformity of the class samples using various pre-processing techniques and to prepare the input data to be more consistent and information-rich.
2. In the second phase, t-SNE is employed to project high-dimensional class samples representations into a two-dimensional space while preserving local relationships among these samples, facilitating visual assessment of class separability and proper distribution of samples after deep synthetic oversampling.
3. In the third phase, the convolutional layers are effectively extracts anatomical features based on these successive convolutional blocks. Finally, a dense layers detect multi-stage Alzheimer's disease. The workflow of the proposed approach is shown in Figure 4.

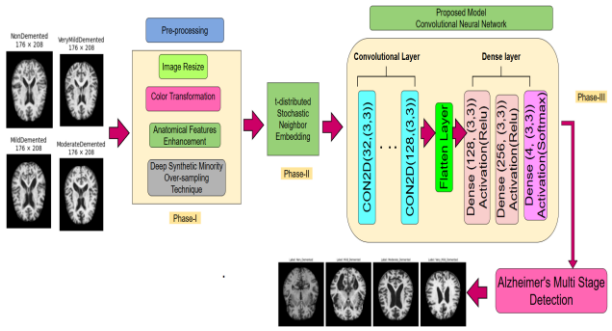


**Figure 4. Workflow of the proposed work.**

### 4.1. Pre-processing

As part of this subsection, the MRI images undergo various pre-processing steps to ensure better consistency and improve image quality. These steps include image resizing, color conversion, fine-tuning of MRI images (e.g., Gaussian kernel, CLAHE, and sharpening), and synthetic minority oversampling. The pre-processing steps are described below:

**Image Resized**

The MRI images are resized from (176 x 208) to (128 x 128) to ensure a more consistent input to the model, enabling better training and more efficient computation, as shown in Figure 5.

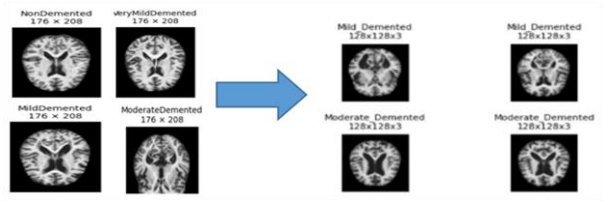


**Figure 5.** Image resized.

**Color Transformation**

Color transformation is required to standardize MRI intensities and enhance tissue contrast, making anatomical features easier for the convolutional neural network to extract features effectively for Alzheimer detection, as shown in Figure 6.

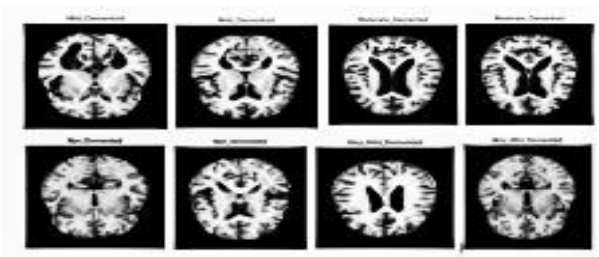

**Figure 6. Enhancement of MRI images using color transformation**

**Anatomical features enhancement**

A Gaussian kernel is used to smooth the MRI image, reducing noise and separating unwanted variations while preserving overall structure, followed by CLAHE to enhance local contrast, making subtle tissue differences more visible for early detection of Alzheimer's disease. Finally, sharpening further emphasizes edges and structural details, aiding the CNN in accurately identifying pathological regions. Together, these three steps produce a cleaner, more precise, and more feature-rich MRI input for the CNN, as shown in Figure 7.

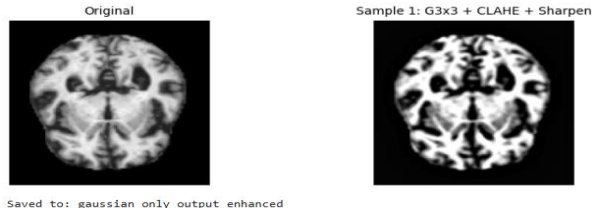


**Figure 7.** Enhanced anatomical features.

To perform better results, the dataset is divided into two sets: a training set and a testing set. 80% of the dataset is allocated for training and 20% for testing. Due to this, the datasets are balanced during the training process.

**Deep synthetic oversampling techniques**

To address class imbalance, the deep synthetic minority over-sampling technique is used to balance the class samples of the minority classes. The following algorithm is used to balance the classes:

Algorithm 1. Deep Synthetic Minority Over-Sampling Technique ($T_{synt}$)

Require: Minority class samples $T_{min}$, number of synthetic samples N, number of nearest neighbors k
Ensure: Synthetic dataset $T_{synt}$
1: Initialize $T_{synt} \leftarrow \emptyset$
2: **for all** $T_i \in T_{min}$ do
3: Find k nearest neighbors of $T_i$ from $T_{min}$, excluding $T_i$
4: **for** n = 1 to N/k do
5: Randomly select one neighbor $T_j$
6: Balance sample:
$T_{new} = T_i + \lambda (T_j - T_i)$, $\lambda \in [0, 1]$
7: Add $T_{new}$ to $T_{synt}$
8: **end for**
9: **end for**
10: **return** $T_{synt}$

Let $T_{min}$ denote the collection of samples from the minority class. For each MRI image sample $T_i \in T_{min}$, this technique finds its k nearest neighbors within the same class. A random selection of these neighbors is then used to generate new synthetic samples. Each new sample $T_{new}$ is produced by interpolating between $T_i$ and one of its neighbors $T_j$ using equation (1):

$$T_{new} = T_i + \lambda \cdot (T_j - T_i),\ \lambda \in [0,1] \quad (1)$$

This procedure is repeated until the desired number N of synthetic samples is generated. The outcome is an expanded and more balanced dataset, $T_{synt}$, which helps improve class distribution, especially in Alzheimer's disease detection. The total number of samples is balanced before and after SMOTE during training set, as shown in Table 1.

**Table 1: Balancing the class samples before and after SMOTE during training**

| Class | Before Balancing Training Samples | After Balancing Training Samples |
|---|---|---|
| Mild demented | 717 | 2560 |
| Moderate Demented | 51 | 2560 |
| Non Demented | 2560 | 2560 |
| Very Mild Demented | 1792 | 2560 |

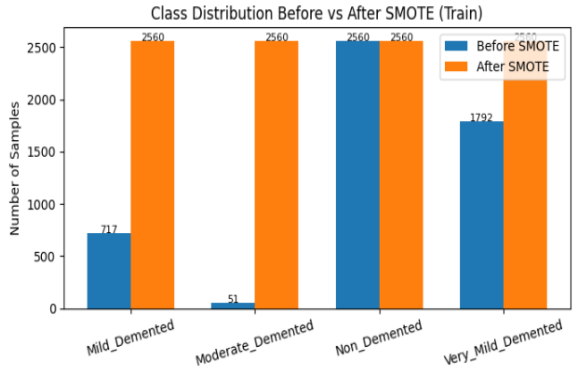


**Figure 8. Class samples balanced during training**

**t-Distributed Stochastic Neighbor Embedding (t-SNE)**

Figure 9 shows a visualization of four classes. t-SNE arranges images in a two-dimensional space based on how similar their raw pixel patterns are, using the Euclidean distance to measure similarity. For every pair of images, t-SNE computes the Euclidean distance between their pixel-intensity vectors; images with small distances are considered similar and are placed close together, while those with large distances are pushed farther apart. As a result, Non-Demented, Very Mild, and Mild Demented images appear strongly overlapped because their Euclidean distances are relatively small. Thus, the subtle structural differences among these early stages are not substantial enough in raw pixel form to produce separable clusters. Moderate Demented images, although more visually distinct, still do not form a clear, isolated cluster because pixel-level Euclidean differences alone cannot fully capture the more profound anatomical changes associated with advanced disease using equation (2).

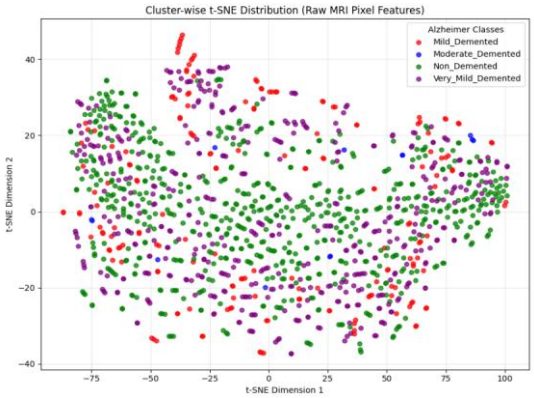


**Figure 9. Visualization of class samples.**

$$d(x_i, x_j) = \sqrt{\sum_{l=1}^{n} (x_{il} - x_{jl})^2} \quad \text{t-SNE} \quad (2)$$

In order to identify similarities and differences among class samples representations across various classes, the pairwise matrix is used. It ranges from 0 to 1, with a value of 1 indicating the highest degree of similarity (almost overlapping features), and a value near 0 indicating a minimal level of similarity (clearly distinguishable patterns). The results show that Non-Demented and Very Mild Demented have the most significant similarity (0.96), suggesting that the earliest degenerative changes in Very Mild Dementia remain visually similar to healthy brain structure. Also, Mild Demented is strongly similar to Non-Demented (0.85) and Very Mild Demented (0.82), suggesting that mild symptoms share some structural similarities to early-stage or healthy MRI features. As shown in Figure 10, Moderate Demented shows low similarity to all other stages (0.00–0.11), indicating that its brain features are distinct and easy to distinguish.

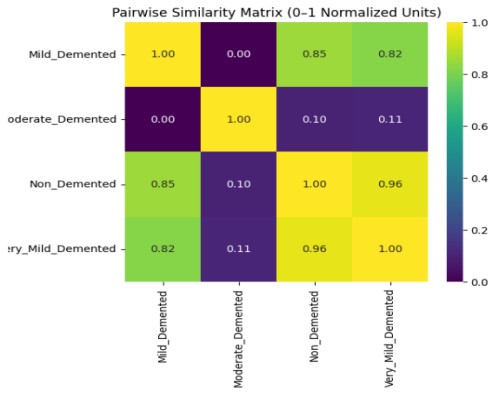


**Figure 10. Normalized class samples.**

**Proposed model for detection of multi stage Alzheimer's disease**

A proposed model comprising two main components: a convolutional layer for feature extraction and finally, a dense layer for Alzheimer's multi-stage detection. The pseudocode of the proposed model is shown below:

Pseudocode 1. Convolutional Neural Network for detection of Alzheimer disease

Require: Input MRI image I, image size = 128×128×3, learning rate $l_r$=1e−4, number of output classes C=4
Ensure: Predicted Alzheimer class label ŷ

1. Initialize CNN model M as Sequential.
2. Input image I and normalize pixel values to [0,1].
3. Feature Extraction Blocks:

**BLOCK–1**

i. Add Conv2D (32 filters, kernel 3×3, ReLU, same padding).
ii. Add Batch Normalization.
iii. Add MaxPooling2D with pool size 2×2.

**BLOCK–2**

i. Add Conv2D (64 filters, 3×3, ReLU).
ii. Add Batch Normalization.
iii. Add MaxPooling2D (2×2).

**BLOCK–3**

i. Add Conv2D (128 filters, 3×3, ReLU).
ii. Add Batch Normalization.
iii. Add MaxPooling2D (2×2).

**BLOCK–4**

i. Add Conv2D (256 filters, 3×3, ReLU).
ii. Add Batch Normalization.
iii. Apply MaxPooling2D (2×2).

**Dense Head:**

i. Flatten feature maps.
ii. Add Dense layer (256 units, ReLU, dropout (0.4)).
iii. Add Dense layer (128 units, ReLU, dropout (0.3)).
iv. Add final Dense layer with Softmax activation for C=4 output classes.

5. Train the model on the SMOTE-balanced dataset.
6. Predict class ŷ = argmax(ŷ(Softmax(M(I)))).
7. Return detected Alzheimer disease.

The network begins with four convolutional blocks, each containing a Conv2D layer followed by ReLU activation, batch normalization, and max-pooling (2×2). As the MRI data moves from Block-1 to Block-4 and the number of filters increases from 32 to 256, enabling the model to learn progressively deeper spatial features, the model is initialized with simple edges, boundaries, shapes, and textures. It progresses towards advanced, complex Alzheimer's related structural patterns within the brain. Now, in (Block-1), it extracts low-level spatial features, including edges, texture, and the overall brain outline. Moving to (Block-2), the network begins to capture more refined structural information, including more apparent tissue density variations and improved grey–white matter separation. Moving towards Block-3, the features transition to mid-level representations to extract structural changes, such as cortical thinning, hippocampal changes, and other neurodegeneration-related complex patterns, where early signs of neurodegeneration become more identifiable in the extracted patterns. As a result of this transformation, the model can identify subtle disease markers across low- and high-level features. As a final step, Block-4 indicates how CNN filters and compresses information to detect multi-stage Alzheimer's disease by retaining only the most discriminative and disease-relevant regions. Once the extracted features have been mapped, they are sent to the dense head, where layers with 256 and 128 neurons are connected and regularized with dropout to refine high-level features as shown in Figure 11.

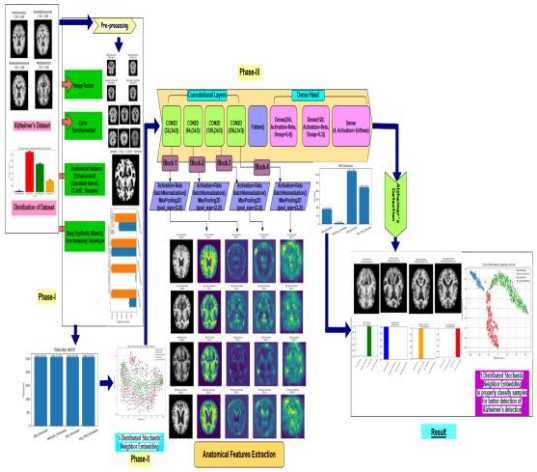


**Figure 11. Proposed Architecture of Alzheimer's disease detection.**

## 5. Result and discussion

In this section, the proposed model is evaluated using a confusion matrix, which provides insight into correct and incorrect predictions across the four Alzheimer's disease classes and highlights specific misclassification patterns. Other assessments, such as performance, are based on accuracy, precision, recall, and F1-score. Finally, the last section compares the proposed model with other existing models.

### Confusion matrix

During execution of the proposed model at 35 epochs, a strong diagonal pattern indicates that the model accurately predicted the majority of samples in each class. All 179 samples were correctly classified as Mild Demented, with no misclassifications. In addition, 13 samples were accurately identified as moderate demented, reflecting that this stage is highly separable. Further, the Non-Demented class was perfectly classified, with 622 correct predictions and only 4 misclassifications, all of which were predicted as mild, and 14 as very mild, based on subtle structural similarities in early-stage dementia. A total of 434 samples were correctly classified as very mild demented, with minor confusion: 6 were misclassified as Mild, while 8 were misclassified as Non-Demented, as shown in Figure 12. Given the borderline nature of this stage, this is not surprising. Additional metrics, such as precision, recall, and F1-score, are included to better assess the model's performance across all classes.

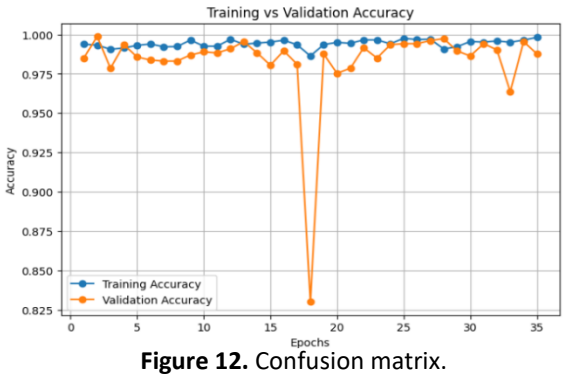


**Figure 12.** Confusion matrix.

### Performance assessment

The proposed model is trained with millions of parameters in conjunction with the Adam optimizer, an optimization algorithm that updates the network's weights during training. By efficiently adjusting weights based on gradients, it minimizes the loss function. By using a mathematical representation [15], the model learns faster, converges smoothly, and does not get stuck in poor local minima, which improves its overall performance:

$$m_t = \beta_1 m_{t-1} + (1-\beta).g \quad (3)$$

$$v_t = \beta_2 v_{t-1} + (1-\beta).g^2 \quad (4)$$

$$weight\ (t) = weight_{t-1} - \left(\frac{\alpha}{\sqrt{\bar{v}+\epsilon}}\right).\bar{m} \quad (5)$$

Where, $m_t$ and $v_t$ stand for the moving averages of the gradients and squared gradients, respectively, that are exponentially weighted. While β1 and β2 are decay rate parameters, $\bar{m}$ and $\bar{v}$ are bias-corrected estimates of the moments. The trainable parameters are 4,617,348, and the non-trainable parameters are 960. The model shows consistently high training accuracy, remaining close to 1.0 throughout, indicating effective learning of discriminative MRI features.

Now in the validation phase, the accuracy remains high and stable, with only minor fluctuations, suggesting reasonable generalization to unseen data. A single sharp drop observed around Epoch 19 indicates a temporary instability in validation performance. The accuracy of validation quickly recovers and aligns closely with the training curve once the optimization is complete. This is normal during optimization. The proposed model is now verified to have an accuracy of 97.97% and an average time of 6.36 seconds, as shown in Figure 13. This is a good indicator that the model avoids overfitting and maintains reliable performance.

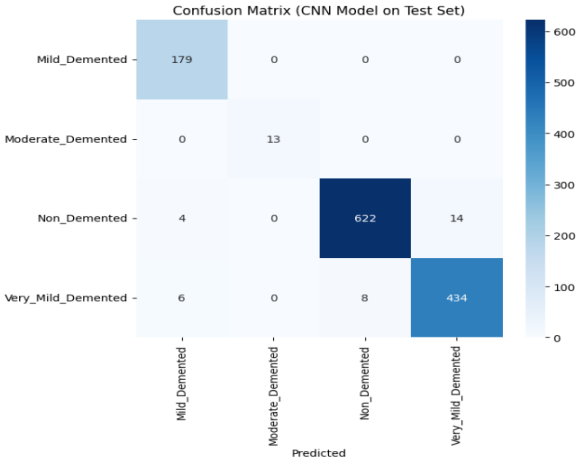


**Figure 13**. Performance assessment.

$$Accuracy = \frac{TP+TN}{TP+TN+FP+FN} \quad (6)$$

The training loss remains consistent with reasonable loss curves at 35 epochs, which indicates that MRI features can be learned effectively and consistently. In addition, the validation loss also follows a similar pattern with minor fluctuations, which shows excellent generalization to unseen data in this context. It is notable that the loss spikes around epoch 19, indicating that the model was having difficulty adapting to an unknown dataset, but then rapidly returns to its

previous level, indicating that no sustained overfitting occurred.

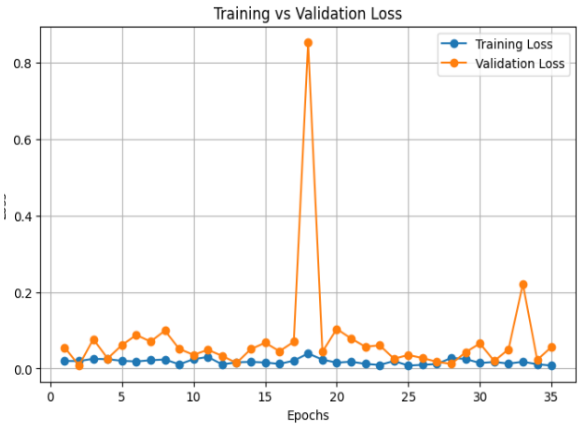


**Figure 14**. Loss assessment.

This model achieves highly reliable, stable classification results across the four Alzheimer classes, as shown in Table 2. A high sensitivity and low false negative rate were observed for Mild Demented cases, with a precision of 0.95, a recall of 1.00, and an F1-score of 0.97. The Moderate Demented class shows perfect precision, recall, and F-score, achieving 100% accuracy, indicating that the model distinguishes this advanced stage with complete reliability. Although there is a slight overlap with early-stage dementia in the Non-Demented case, the model achieved 0.99 precision, 0.97 recall, 0.98 F-score, and 92.28% accuracy in identifying healthy subjects. Due to the model's ability to detect subtle structural changes early on, Very Mild Demented images consistently achieved high performance, with 0.97 precision, 0.97 recall, 0.97 F1-score, and 96.88% accuracy.

**Table 2:** Class-wise performance assessment

| Class | Precision | Recall | F1_score | Accuracy (%) |
|---|---|---|---|---|
| Mild demented | 0.95 | 1.00 | 0.97 | 99.46 |
| Moderate demented | 1.00 | 1.00 | 1.00 | 100 |
| Non demented | 0.99 | 0.97 | 0.98 | 92.28 |
| Very mild demented | 0.97 | 0.97 | 0.97 | 96.88 |

$$Precision = \frac{\mathrm{TP}}{\mathrm{TP} + \mathrm{FP}} \quad (7)$$

$$Recall = \frac{\mathrm{TP}}{\mathrm{TP} + \mathrm{FN}} \quad (8)$$

$$F1\_score = \frac{2 * Precision * Recall}{Precision + Recall} \quad (9)$$

A t-SNE plot indicates that the proposed model efficiently separates Alzheimer's disease classes into distinct clusters based on their learned feature embedding's, as shown in Figure 15. It shows that the CNN captures meaningful structural differences in MRI scans by forming well-defined groups with minimal overlap, such as Mild, Moderate, Non-Demented, and Very Mild cases. This strong cluster separation indicates that the model can learn discriminative features necessary for accurately identifying Alzheimer's stages. N=200 samples take 0.66 seconds to run, 400 samples take 1.21 seconds to run, 800 samples take 2.59 seconds to run, and 1280 samples take 4.05 seconds to run.

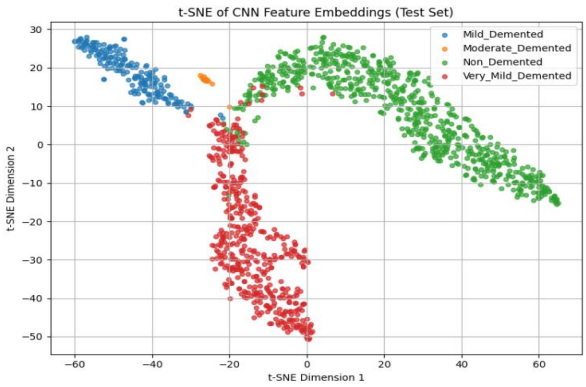


**Figure 15**. Class-wise separation of anatomical Feature.

### 6. Conclusion and Future Scope

This paper proposes a convolutional neural network-based model for detecting Alzheimer's disease. MRI image quality and consistency are improved through various pre-processing steps, ensuring the model learns disease-related mean features. The proposed approach, in conjunction with the Adam optimizer, performs hierarchical feature extraction, moving from fine structural details to coarse discriminative patterns, enabling

better separation of Alzheimer's stages. Additionally, t-SNE visualization is employed to verify that the model is learning meaningful anatomical distinctions, providing an intuitive assessment of how well the model differentiates between disease severity classes. The performance is measured by precision, recall, and F1_score, which have improved, resulting in an accuracy of 97.97% and demonstrating the model's robustness.

In future work, to test for ventricular enlargement, which is characterized by an abnormal increase in the size of the brain's ventricles caused by the loss or shrinkage of surrounding brain tissue, we plan to collect real-time Alzheimer's datasets and apply other deep learning models.

**References**

[1] Abdul Azeem, Y., Bahgat, W. M., & Badawy, M. (2021). A CNN based framework for classification of Alzheimer's disease. Neural Computing and Applications, 33(16), 10415-10428.

[2] Tufail, A. B., Ma, Y. K., & Zhang, Q. N. (2020). Binary classification of Alzheimer's disease using sMRI imaging modality and deep learning. Journal of digital imaging, 33(5), 1073-1090.

[3] Dementia. (n.d.) https://www.who.int/news-room/fact-sheets/detail/dementia. Accessed 07 Apr 2022.

[4] World Alzheimer Report 2021 | Alzheimer's Disease International (ADI)." (n.d.) https://www.alzint.org/resource/world-alzheimer-report-2021/. Accessed 08 Apr 2022.

[5] Turkson, R. E., Qu, H., Mawuli, C. B., & Eghan, M. J. (2021). Classification of Alzheimer's disease using deep convolutional spiking neural network. Neural Processing Letters, 53(4), 2649-2663.

[6] Alzheimer's stages: How the disease progresses - Mayo Clinic. (n.d.) https://www.mayoclinic.org/diseases-conditions/alzheimers-disease/in-depth/alzheimers-stages/art-20048448. Accessed 07 Apr 2022.

[7] NIH-MedlinePlus, https://www.nlm.nih.gov/medlineplus/magazine/issues/fall10/articles/fall10pg20-21.ht, Oct'2011.

[8] Shanmugam, J. V., Duraisamy, B., Simon, B. C., & Bhaskaran, P. (2022). Alzheimer's disease classification using pre-trained deep networks. Biomedical Signal Processing and Control, 71, 103217.

[9] Shanmugam, J. V., Duraisamy, B., Simon, B. C., & Bhaskaran, P. (2022). Alzheimer's disease classification using pre-trained deep networks. Biomedical Signal Processing and Control, 71, 103217.

[10] Zeng N, Li H, Peng Y (2021) A new deep belief network-based multi-task learning for diagnosis of Alzheimer's disease. Neural Comput Applic. https://doi.org/10.1007/s00521-021-06149-6.

[11] Jing, H. (2020). How Convolutional Layers Work in Deep Learning Neural Networks? Jingles, Github Blog.

[12] Tripathy, S. K., Nayak, R. K., Gadupa, K. S., Mishra, R. D., Patel, A. K., Satapathy, S. K., ... & Barsocchi, P. (2024). Alzheimer's disease detection via multiscale feature modelling using improved spatial attention guided depth separable CNN. International Journal of Computational Intelligence Systems, 17(1), 113.

[13] Alatrany, A. S., Khan, W., Hussain, A., Kolivand, H., & Al-Jumeily, D. (2024). An explainable machine learning approach for Alzheimer's disease classification. Scientific reports, 14(1), 2637.

[14] Shaffi, N., Viswan, V., & Mahmud, M. (2024). Ensemble of vision transformer architectures for efficient Alzheimer's Disease classification. Brain Informatics, 11(1), 25.

[15] Rana, M. M., Islam, M. M., Talukder, M. A., Uddin, M. A., Aryal, S., Alotaibi, N., ... & Moni, M. A. (2023). A robust and clinically applicable deep learning model for early detection of Alzheimer's. IET Image Processing, 17(14), 3959-3975.

[16] Kohli, N., & Kumar, T. (2023). Envisaging Alzheimer's Disease Stage through Fuzzy Rank-Based Ensemble of Transfer Learning Models. International Journal of Performability Engineering, 19(6), 397.

[17] Kamath, D., Fathima, M. F., & Mohanchandra, K. (2021). Early Detection of Alzheimer's Disease using Convolutional Neural Network Architecture. International Journal of Artificial Intelligence, 8(2), 48-57.

[18] Nagarathna, C. R., & Kusuma, M. (2022). Automatic diagnosis of Alzheimer's disease using hybrid

model and CNN. Journal of Soft Computing Paradigm, 3(4), 322-335.

[19] Mmadumbu, A. C., Saeed, F., Ghaleb, F., & Qasem, S. N. (2025). Early detection of Alzheimer's disease using deep learning methods. Alzheimer's & Dementia, 21(5), e70175.

[20] Pinamonti, M. (2025). Alzheimer MRI 4 classes dataset. Kaggle.

[21] Sachin Kumar, Alzheimer MRI Pre-processed Dataset, https://www.kaggle.com/datasets/sachinkumar413/alzheimer-mri-dataset,2022, Accessed on 15 April 2023.

[22] Alzheimer's Disease Neuroimaging Initiative (ADNI),https://adni.loni.usc.edu/data-samples/access-data/, Accessed on 18 May 2021.

[23] Rosen, W. G., Mohs, R. C., & Davis, K. L. (1984). A new rating scale for Alzheimer's disease. The American journal of psychiatry, 141(11), 1356-1364.